Nuclear Engineering and Design 418 (2024) 112899

Contents lists available at ScienceDirect

Nuclear Engineering and Design

journal homepage: www.elsevier.com/locate/nucengdes

JENDL-5.0 nuclear data sensitivity, uncertainty, and similarity analyses on the criticality of RSG GAS multipurpose research reactor

Peng Hong Liem [a,b,*], Donny Hartanto [c]

[a] Cooperative Major in Nuclear Energy, Graduate School of Engineering, Tokyo City University (TCU), 1-28-1 Tamazutsumi, Setagaya, Tokyo, Japan
[b] Scientific Computational Division, Nippon Advanced Information Service (NAIS Co., Inc.), 416 Muramatsu, Tokaimura, Ibaraki, Japan
[c] Oak Ridge National Laboratory, One Bethel Valley Road, Oak Ridge, TN 37830, USA

ARTICLE INFO

Keywords:
JENDL-5.0
S/U & similarity analysis
RSG GAS multipurpose reactor
Covariance matrices
AMPX-6

ABSTRACT

The criticality, sensitivity, uncertainty and similarity analysis of the clean, first core of the G. A. Siwabessy Multipurpose Reactor (RSG GAS), using the newly released Japanese Nuclear Data Library version 5 (JENDL-5) was conducted to contribute the validation effort of the JENDL-5, especially for the application on beryllium reflected, light-water moderated, low-enriched uranium (19.75 wt%) fueled material testing reactors. The JENDL-5 sensitivity coefficients and covariance matrices were prepared by MCNP6 and AMPX-6, respectively. The keff uncertainty was then evaluated with TSUNAMI-IP module of SCALE-6. The same module was used for similarity analysis by comparing the sensitivity data of 3,690 criticality experiments. The criticality (keff) analysis results ([C/E-1]) showed maximum overestimation of 801 pcm, 477 pcm and 547 pcm, for JENDL-5, JENDL-4.0 and ENDF/B-VIII.0, respectively. The keff uncertainty originated from the nuclear data was estimated to be 620 pcm, 644 pcm and 637 pcm for JENDL-5 only, JENDL-5 & ENDF/B-VIII.0, and ENDF/B-VIII.0 covariance data, respectively, which are comparable with the keff ([C/E-1]) values. About 125 experiment cases were found to have correlation factors of > 0.8, however, no experiment showed a strong correlation factor (>0.9), therefore, in the future criticality experiments similar to the RSG GAS should be conducted.

1. Introduction

Almost twelve years after the Japanese Evaluated Nuclear Data version 4 (JENDL-4.0) was released (2012) (Shibata et al., 2011), the new version, i.e., the JENDL-5, was released in December 2021 (Iwamoto et al., 2023)). The new release was mainly aimed to contribute to the existing important issues on nuclear energy development in Japan (Iwamoto et al., 2020). The issues include the treatment of nuclear waste and the enhancement of nuclear safety. Related to the present work, it is worthily noted that the new JENDL-5 provides a neutron-induced reaction data sub-library from H (Z = 1) to Fm (Z = 100) for 795 nuclides and a thermal-scattering law (TSL) sub-library for 37 materials (covering 62 elements). To appreciate the significance of the new release, for comparison, the previous version, JENDL-4.0, provides a neutron-induced reaction data sub-library for only 406 nuclides and a TSL sub-library only for 15 materials. For nuclear data uncertainty evaluation, reliable covariance data are essential. The newly released JENDL-5 provides more covariance data than the previous version (JENDL-4.0); however, as will be reported later, the provided covariance data of some important nuclides are still missing for the present application.

In our previous works, the criticality experiments of the clean, first core of the G. A. Siwabessy Multipurpose Reactor (RSG-GAS) were used to validate the JENDL and other worldwide used nuclear data libraries (ENDF and JEFF). The RSG GAS is a light water-moderated and cooled material testing reactor that uses beryllium as its neutron reflector. It is designed with a maximum thermal power of 30 MW. The first criticality of this reactor was achieved in July 1987, and it reached 30 MW of power after going through 6 transition cores. Initially, this reactor used a material testing reactor (MTR type) oxide fuel (U_3O_8-Al) with low enrichment, 19.75 w/o U-235. To improve the performance of the reactor, the RSG-GAS core was then converted to silicide fuel (U_3Si_2-Al) first with the same uranium density, 2.96 g/cm^3, and in the future with higher uranium densities. The new equilibrium silicide core was proposed and designed by Liem et al. (1998). The transition cores from oxide to silicide have been also investigated, and the transition strategies were established by Liem and Sembiring (2010). Based on the proposed strategies, the conversion work was started by operating a series of

* Corresponding author at: Scientific Computational Division, Nippon Advanced Information Service (NAIS Co., Inc.), 416 Muramatsu, Tokaimura, Ibaraki, Japan.
E-mail address: liemph@nais.ne.jp (P.H. Liem).

https://doi.org/10.1016/j.nucengdes.2024.112899
Received 13 September 2023; Received in revised form 19 November 2023; Accepted 1 January 2024

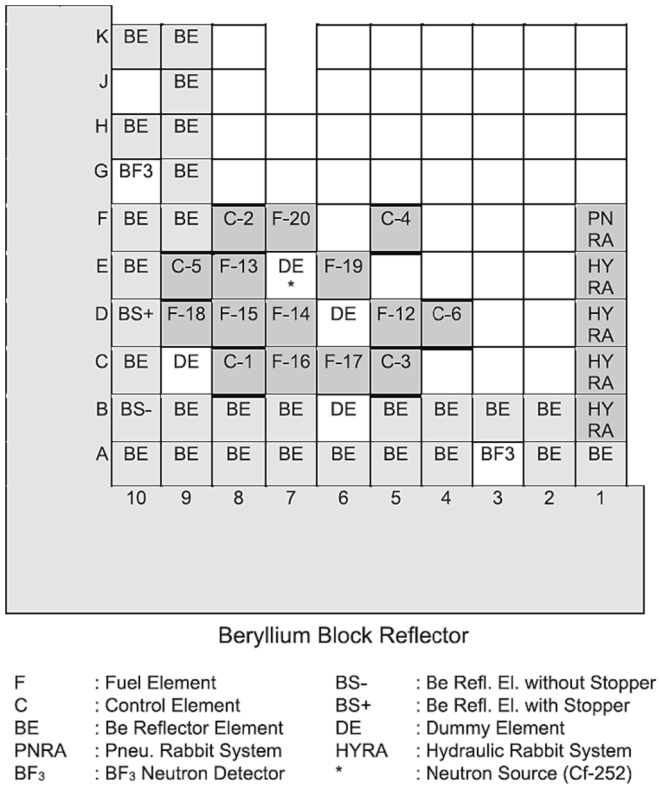

Fig. 1. First criticality core configuration of the RSG GAS first core (modified from Reference (Liem and Sembiring, 2012)).

mixed oxide-silicide cores (Sembiring et al., 2001). A full silicide core has been achieved at Core No. 45 after going through 10 cycles of transition (mixed) oxide-silicide core operation as planned.

The accuracy of the JENDL-3.3 and JENDL-4.0 were validated against the clean, first core of RSG GAS by using the continuous energy Monte Carlo MVP-II code (Nagaya et al., 2005), and the results were reported by Liem (1995), Liem (1998) and Liem and Sembiring (2012), respectively. In these particular works, we only validated the nuclear data against the criticality (multiplication factor, keff) experiments, and no sensitivity analysis (S/A) nor uncertainty analysis (U/A) was conducted. The JENDL-4.0 showed an excellent agreement with the keff overestimation of only ~ 0.2 % and was better than the older JENDL-3.3 (~0.3 %). The S/A of JENDL-4.0 on the first core of RSG GAS criticality was for the first time conducted by using the continuous energy Monte Carlo MCNP-6.2 (Werner et al., 2017) and reported by Liem et al. (2019a), Liem et al. (2019b). To cope with the smaller number of the JENDL-4.0 covariance data, we conducted the U/A using the then-available ENDF/B-VII.1 covariance data (Chadwick et al., 2011). It should be noted that covariance data were compiled into 44 energy groups, and not all of them were of high quality. The S/A for both JENDL-4.0 and ENDF/B-VII.1 showed consistent results in terms of dominant nuclides and their sensitivity values. The large negative sensitivities were found in the (n, gamma) reaction of H-1, U-235, Al-27, U-238, and Be-9. In contrast, large positive sensitivities were found in U-235 (total nu and fission), H-1 (elastic), Be-9 (free gas, elastic), and H-1 (lwtr.20 t, inelastic). The U/A result of ENDF/B-VII.1 showed that the uncertainty of the nuclear data against the keff was approximately 0.6 % which was comparable with the [C/E – 1.0] values of keff. With the similar state of the art of JENDL-4.0 and ENDF/B-VII.1, we expected that the uncertainty of JENDL-4.0 would be in the same order of magnitude.

As a continuation of our previous work, in the present work, we conducted the same S/A and U/A for the newly released JENDL-5.0. As mentioned before, compared to the previous JENDL-4.0, a significantly increased number of high-quality covariance data are available for the release; therefore, we utilized all the available JENDL-5.0 covariance data for the present U/A. Covariance data that were not provided by the JENDL-5.0 release were prepared from the ENDF/B-VIII.0 nuclear data (Brown et al., 2018). The justification is as follows. First, we considered that presently the JENDL-5.0 and the ENDF/B-VIII.0 are in a similar state-of-the-art, and the covariance data are expected to be consistent with each other. Second, before the present work, we conducted validation of the ENDF/B-VIII.0 nuclear data against the same criticality experiments (Hartanto et al., 2019; Hartanto and Liem, 2020). The validation results (keff) showed that the ENDF/B-VIII.0 had the same order of accuracy compared to the then-available JENDL-4.0 and ENDF/B-VII.1. To improve the accuracy of the evaluated uncertainty, the sensitivity profiles and the covariance data were prepared into 252 energy-group and 56 energy-group, respectively. We also generate a special JENDL-5 covariance matrix with additional ENDF/B-VIII.0 covariance data for JENDL-5 nuclides which have no covariance data.

The similarity analysis is never conducted for the RSG GAS although up to the present thousands of high-fidelity critical experiments have been compiled into databases available for the analysis, such as ICSBEP Handbook (OECD/NEA, 2016) and IRPhEP Handbook (OECD/NEA, 2017).

Through the present work, we expect that one can (1) estimate better the JENDL-5.0 dominant nuclides and their reactions which have significant sensitivity against the keff, (2) estimate the uncertainty of JENDL-5.0 against keff and its dependency on the used covariance data, (3) some helpful information as the feedback to the JENDL evaluators and experts for further improvement in the future, (4) whether criticality experiments similar to the RSG GAS are adequately available or similar criticality experiments are needed in the future. Of course, one should be reminded that although the above-mentioned expectation is mainly valid for this particular type of reactor, some educated extrapolation of the results could be useful for reactors with similar neutron spectra and/or reactors with similar fuel compositions.

The manuscript is organized as follows. First, the RSG GAS first core criticality experiments are briefly discussed, followed by the methodology used in the present S/U and similarity analysis. After the criticality, S/U, and similarity analysis results are presented and discussed, the concluding remarks are given.

2. Criticality experiments

The RSG GAS is a light-water moderated and cooled, pool-type MTR that uses beryllium (Be) as its neutron reflector. It is designed with a maximum thermal power of 30 MW. The first criticality of this reactor was achieved in July 1987. The first core used an MTR plate-type oxide fuel (U_3O_8-Al) with low enrichment, 19.75 wt% U-235 (at present the core has been converted to silicide fuel). Figs. 1 and 2 show the first criticality and full core configurations of the first core of RSG GAS, respectively. The main reactor data for the first core is shown in Table 1 and the criticality configurations are summarized in Table 2. The standard fuel element (FE) and the control fuel element (CE) are shown in Figs. 3 and 4, respectively. Other main specifications of the reactors, as well as the details of the criticality experiments, can be found elsewhere (Liem and Sembiring, 2012; BATAN, 1980).

There were two groups of criticality experiments conducted for the first core of RSG GAS, i.e. (1) the criticality approach experiment for achieving the first criticality and the criticality experiment for core excess reactivity loading, and (2) control rod calibrations under critical full core conditions. The first criticality was achieved at the 9-th loading of standard fuel element (Liem and Sembiring, 2012), i.e. the regulating rod (RR) was pulled out slowly (reactor periods were greater than 50 s) while the other 5 shim rods were fully withdrawn. The insertion position of the RR at the first criticality was 475 mm. This configuration, shown in Fig. 1, was chosen as one of the most appropriate for this study. Following the first criticality, the loading of additional fuel elements and reflector elements was conducted to achieve a full core configuration

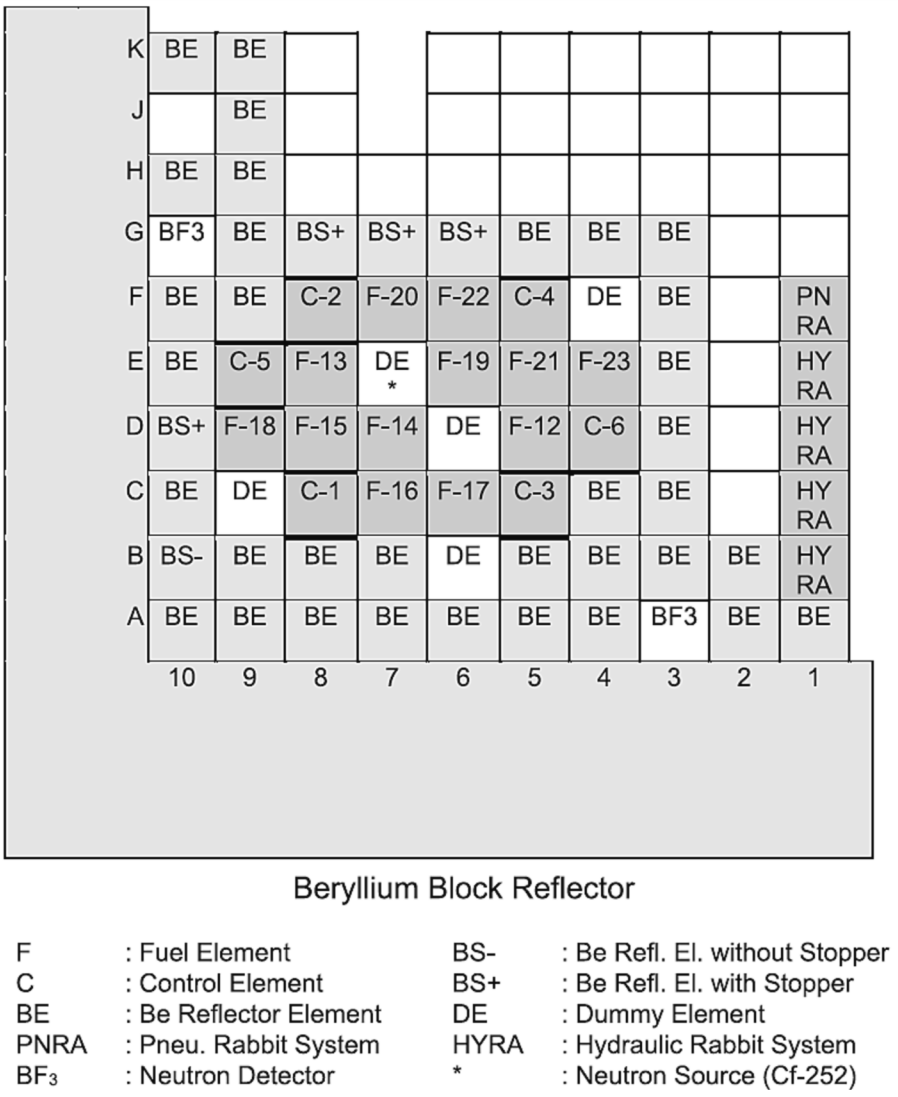

Fig. 2. Full core configuration of the RSG GAS first core (modified from Reference (Liem and Sembiring, 2012)).

(Fig. 2) with sufficient excess reactivity for one core cycle. The reactivity gains were measured at each loading step by calibrating the difference of the regulating rod position with a reactivity meter (compensation method with the other 5 shim rods in bank configuration). The measurement of the accumulated excess reactivity by this method should be considered as an uncorrected value. The excess reactivity value was then corrected by a method described elsewhere (Liem and Sembiring, 2012). In the second group experiments, the control rod calibrations were conducted following the excess reactivity loading for the six control rods with various methods. Many combinations of control rod positions can be found during the calibrations which gave a critical core condition. In this work, the combinations of control rod positions that occurred during control rod calibration with the bank compensation method were selected for the benchmark calculations. Case 2-1 of the second group is selected for the S/U analysis.

3. Methodology

3.1. Sensitivity, uncertainty, and similarity analysis

The calculation flow of the S/U and similarity analysis is shown in Fig. 5. The calculation flow is not specific to JENDL-5 but is also applied to JENDL-4.0 and ENDF/B-VIII.0 evaluated nuclear data libraries. Hereafter, the explanation is focused on the JENDL-5 evaluated nuclear data library.

The sensitivity data, i.e. the sensitivity coefficients ($S_{k,\alpha}$) in 252 energy-group are prepared using the MCNP-6.2 (Werner et al., 2017) code with the KSEN option. The KSEN option is based on the linear perturbation theory with an adjoint weighting function (Kiedrowski and Brown, 2013):

$$S_{k,\alpha} = \frac{\alpha}{keff}\frac{\partial keff}{\partial \alpha} = -\frac{\langle \varphi^{+}, \left(\Sigma_{\alpha} - \mathrm{S}_{\alpha} - \frac{1}{keff}\mathrm{F}_{\alpha}\right), \varphi\rangle}{\langle \varphi^{+}, \frac{1}{keff}\mathrm{F}_{\alpha}\varphi\rangle},$$

where φ and φ^{+} are the forward and adjoint neutron flux; Σ_{α} is the α-type macroscopic cross-section; S_{α} and F_{α} are the scattering and fission operators, respectively; *keff* is the eigenvalue (effective neutron multiplication factor). The $\langle\rangle$ operator is the integration of space and energy domains. Considering the reaction types (α), in the present version of MCNP-6.2, the KSEN option can provide reaction types as shown in Table 3. MCNP-6.2 does not solve the adjoint flux directly, instead, it uses the Iterated Fission Probability method to compute the adjoint-weighted integrals for the sensitivity coefficients (cf. Eq. (1)). For inter-library comparison, the sensitivity profiles were prepared for JENDL-5, JENDL-4.0, and ENDF/B-VIII.0.

The covariance data, i.e. the covariance matrices (***C***), in COVERX 56

Table 1
Main design data of RSG GAS (Liem and Sembiring, 2012).

Reactor Type	Pool Type
Fuel Element Type	LEU Oxide MTR
Moderator/Coolant	H_2O
Reflector	Be & H_2O
Nominal Power (MWth)	10.7
No. of Fuel Elements	12
No. of Control Elements	6
No. of Fork Type Absorber (pairs)	6
Fuel/Control Element Dimension (mm)	77.1 × 81 × 600
Fuel Plate Thickness (mm)	1.3
Coolant Channel Width (mm)	2.55
No. of Plate per Fuel Element	21
No. of Plate per Control Element	15
Fuel Plate Clad Material	$AlMg_2$
Fuel Plate Clad Thickness (mm)	0.38
Fuel Meat Dimension (mm)	0.54 × 62.75 × 600
Fuel Meat Material	U_3O_8-Al
U-235 Enrichment (wt. %)	19.75
Uranium Density in Meat (g/cm^3)	2.96
U-235 Loading per Fuel Element (g)	250
U-235 Loading per Control Element (g)	178.57
Absorber Meat Material	Ag-In-Cd
Absorber Thickness (mm)	3.38
Absorber Clad Material	SUS-321
Absorber Clad Thickness	0.85

Table 2
Criticality and S/U analysis cases.

Case	First criticality and excess reactivity loading (First Group)	Reactor Condition
1-1	First criticality (9 FEs, 6 CEs, RR = 475 mm)	Critical
1-2	Full core (12 FEs, 6 CEs, CRs all up)	Supercritical
1-3	Full core (12 FEs, 6 CEs, CRs all down)	Subcritical
Case	Calibrated rod/grid position (calibrated rod position/other rod bank position) (Second Group, 12 FEs, 6 CEs)	Reactor Condition
2-1	JDA06 / C-8 (600 mm / 290 mm)	Critical ○
2-2	JDA01 / E-9 (600 mm / 284 mm)	Critical
2-3	JDA03 / F-8 (600 mm / 293 mm)	Critical
2-4	JDA05 / C-5 (600 mm / 288 mm)	Critical
2-5	JDA04 / F-5 (600 mm / 290 mm)	Critical
2-6	JDA07 / D-4 (600 mm / 282 mm)	Critical

○: Selected case for S/U analysis.

energy-group format are prepared by employing the AMPX-6 code (Bostelmann et al., 2021; Wiarda et al., 2016), particularly the PUFF-IV module (Wiarda and Dunn, 2008) is utilized. The 56 energy-group structure is identical to the one used in the SCALE-6.2 (Rearden and Jessee, 2016) 56 energy-group covariance data. The nuclear data parameters (i.e., group-wise nuclide-reaction specific cross sections) are represented by the vector $\boldsymbol{\alpha} := (\alpha_m), m = 1, 2, \cdots, M$, where M is the number of nuclide-reaction pairs × the number of energy groups. The corresponding covariance matrix containing the relative variances and covariances in the nuclear data are

$$\boldsymbol{C}_{\alpha\alpha} := \left[\frac{COV(\alpha_m, \alpha_p)}{\alpha_m, \alpha_p}\right], m = 1, 2, \cdots, M; p = 1, 2, \cdots, M,$$

where

$$COV(\alpha_m, \alpha_p) = \langle \delta\alpha_m, \delta\alpha_p \rangle.$$

The $\delta\alpha_m$ and $\delta\alpha_p$ represent the difference between the values and expectation values of the nuclear data parameters.

For inter-library comparison, the covariance matrices were evaluated for JENDL-5 and ENDF/B-VIII.0. Amongst the 795 nuclides of JENDL-5, only 105 nuclides have covariance data (see Table 4) while the ENDF/B-VIII.0 has 251 nuclides with covariance data. Hence, since the number of JENDL-5 nuclides with covariance data is significantly less than the one of ENDF/B-VIII.0, in the present work we also compiled a special covariance matrix of JENDL-5 with the addition of ENDF/B-VIII.0 covariance data for JENDL-5 nuclides which have no covariance data. Using this special JENDL-5 covariance matrix, the uncertainty of JENDL-5 can also be compared to the one of ENDF/B-VIII.0.

Based on the sensitivity coefficients (Eq. (1)) and covariance matrices (Eq. (2)), the keff uncertainty matrix, $\boldsymbol{U}_{kk}$, can be estimated as

$$\boldsymbol{U}_{kk} = \boldsymbol{S}_k \boldsymbol{C}_{\alpha\alpha} \boldsymbol{S}_k^T$$

where T indicates a transpose. The diagonal elements of the $\boldsymbol{U}_{kk}$ consists of relative variance values, σ^2, and by taking the squared root of these values, i.e., σ, the keff uncertainty for each nuclide-reaction can be obtained. For the calculations of $\boldsymbol{U}_{kk}$ the TSUNAMI-IP module (Rearden and Jessee, 2009) of SCALE-6.3 (Wieselquist et al., 2021) is used. As mentioned above, the uncertainty matrices were calculated for JENDL-5 only, JENDL-5 + ENDF/B-VIII.0, while the ENDF/B-VIII.0 covariance matrices were taken for the SCALE 6.3.

The similarity analysis uses the same TSUNAMI-IP module. The number of criticality experiments taken into account for the present similarity analysis is 3,690 cases, obtained from ICSBEP Handbook (OECD/NEA, 2016). The similarity evaluation is based on the sensitivity coefficients, either alone or in combination with cross-section uncertainty information. The similarity of the RSG GAS core with these criticality experiments is expressed with an index, i.e. correlation factor ($\boldsymbol{c_k}$) which has a range from 0 to 1.0. $\boldsymbol{c_k}$ close to 1.0 indicates a strong correlation, that is, a strong similarity exists between the RSG GAS core and the corresponding criticality experiment. The complete derivation of the $\boldsymbol{c_k}$ can be found in the SCALE/TSUNAMI-IP module manual (Rearden and Jessee, 2009).

3.2. Monte Carlo modeling

The active part (7.71 × 8.1 × 60 cm^3) of both FE and CE were modeled as their exact geometry and dimensions while the top and end-fitting of the elements were modeled approximately since their geometry is very complicated, that is, the structure materials were homogenized with water by volume weighting. An exact modeling approach was also taken for the active parts of the Be reflector elements, Be block elements, and irradiation positions. Considering their complicated geometry, the core grid and bottom support were also treated approximately as for the top or end-fitting of fuel elements. This approximation did not deteriorate the accuracy of calculation results since it was applied in the non-active parts of the core. The movable control rods (absorber blades) were modeled according to their exact geometry and dimensions. Consequently, a 60 cm water layer above the core had to be included in the calculation to provide enough space for the absorber blades when a control rod was fully withdrawn. Approximately 30 cm water layers were included below the core bottom support, and around the beryllium block and element reflectors. Vacuum boundary conditions were imposed on the outer boundary of the reactor system.

All calculations in the present benchmark were conducted with the JENDL-5 library for a room temperature of 300 K. The measured critical effective multiplication factors were corrected when the core isothermal temperature was not identical to 300 K. The total number of batches (generations) was 10,000 where each batch consists of 10,000 histories, i.e. the total number of effective histories was 100 million. Initial 100 batches were skipped to guarantee the fundamental mode had been achieved before statistical evaluation of keff and other tallies were conducted. Under these calculation conditions, the fractional standard deviation (FSD) for keff was less than 0.01 % for all cases. The main benchmark results are the keff values which can be directly compared with the experimental/measured ones. The inter-library comparison results also provide valuable information, differences in the critical keff,

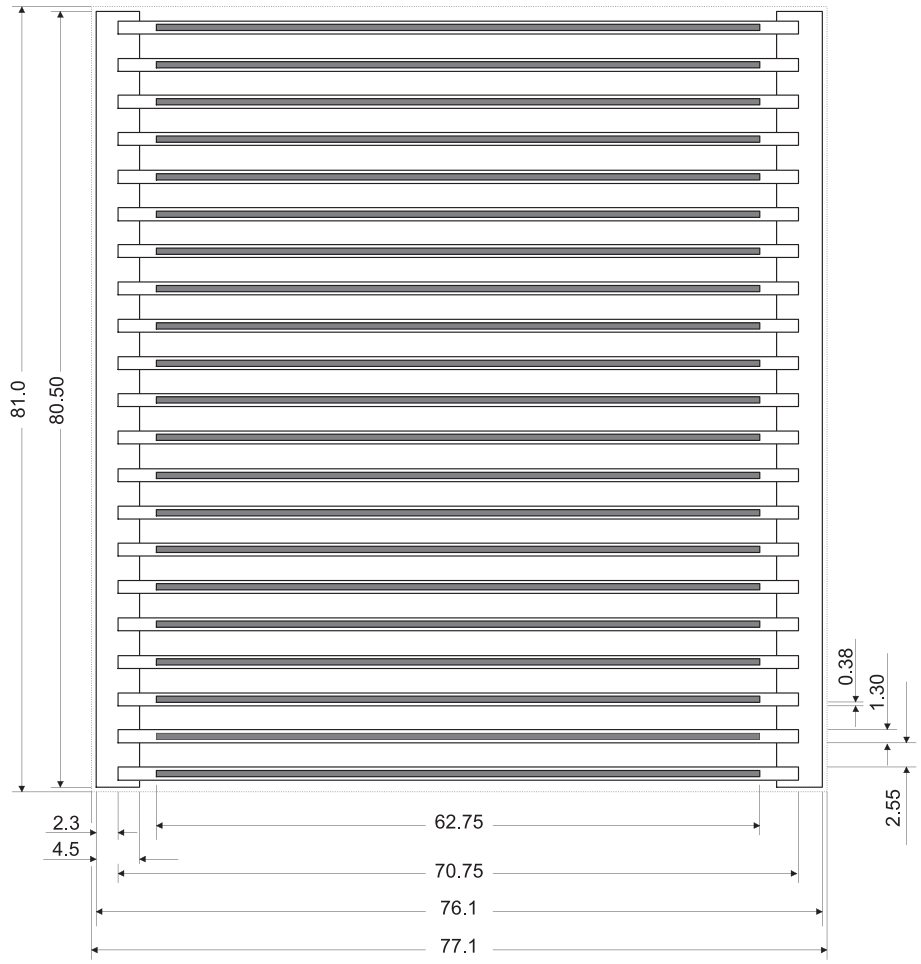

Fig. 3. Standard fuel element (FE) of RSG GAS reactor (unit mm).

excess reactivity, and control rod worth amongst libraries will also be presented and discussed.

4. Analysis results and discussion

4.1. Criticality analysis

The MCNP criticality analysis results for JENDL-5, JENDL-4.0, and ENDF/B-VIII.0 are shown in Table 5, divided into two groups in accordance with Table 2. The experiment/measured keff is 1.0, hence the calculated to experiment (C/E) values can be readily estimated from the table (excluding non-critical cases, 1-2 and 1-3). In general, the JENDL-4.0 results show the closest agreement with the experiment results, followed by ENDF/B-VIII.0 and JENDL-5. Of the first group, the first criticality (Case 1-1) consisted of 9 FEs and 6 CEs, and the core had a small excess reactivity equivalent to the insertion of the regulation rod (RR, position 475 mm). For this first criticality condition, the JENDL-5, JENDL-4.0, and ENDF/B-VIII.0 results (keff) show an overestimation of 801 pcm, 477 pcm, and 547 pcm, respectively. For the second group, 6 cases of critical full core during control rod calibration (Case 2-1 to 2-6) consisted of 12 FEs and 6 CEs, and all control rods were inserted partially, except the measured control rod. For the second group, the maximum overestimation of keff values of JENDL-5, JENDL-4.0, and ENDF/B-VIII.0 were 650 pcm, 431 pcm, and 452 pcm, respectively.

Concerning the inter-library comparison, the following results were observed. The keff values of JENDL-4.0 were considerably close to the ones of the ENDF/B-VIII.0, where the maximum relative difference between the two libraries was only 70 pcm (First group, Case 1-1, first criticality (9 FEs, 6 CEs, RR = 475 mm)). Other cases, i.e. Second group, showed relative differences of less than 50 pcm. The keff values of JENDL-5 differed considerably from the ones of JENDL-4.0 and ENDF/B-VIII.0, where the maximum relative differences were 321 pcm and 252 pcm, respectively (both for Case 1-1, first criticality (9 FEs, 6 CEs, RR = 475 mm)). Other cases, i.e. Second group, showed relative differences of less than 220 pcm and 197 pcm, respectively. The keff differences between the JENDL-5 and previous JENDL-4.0 showed the same order and trend as reported in Table 4 of Tada et al. (2023). The table shows the reactivity differences of uranium-fueled light-water-moderated systems when each nuclide is changed from JENDL-5 to JENDL-4.0. The light-water-moderated systems refer to LCT-02-01, LCT02-05, LCT26-01, LCT48-03, LCT48-04, and LCT79-02, where LCT stands for LEU-COMP-THERM (OECD/NEA, 2016). They concluded that the JENDL-5 (C/E) values were within the uncertainty of the (C/E) values for many cases. The difference between JENDL-4.0 and JENDL-5 is from −407 pcm to −9 pcm. They also conducted a 'crude' sensitivity analysis where a single JENDL-5 nuclide was replaced by JENDL-4.0 and the keff difference was evaluated. It was found that the dominant contributors were H in H_2O (TSL), O-16, U-235, and U-238.

In our recent work (Liem and Hartanto, 2023), the above-mentioned crude sensitivity analysis was conducted for the RSG GAS first criticality by using MVP3 code (Nagaya et al., 2016). We found that the main contributors were the nuclides composing the fuel region, i.e. U-235, U-238, and H_2O. Relatively large reactivity changes are observed for U-235, U-238, and water, namely around −50 to −60 pcm. It should be noted that one can not separate the bounded hydrogen S(α,β) thermal library from the free gas (fast) library of MVP libraries, therefore, the

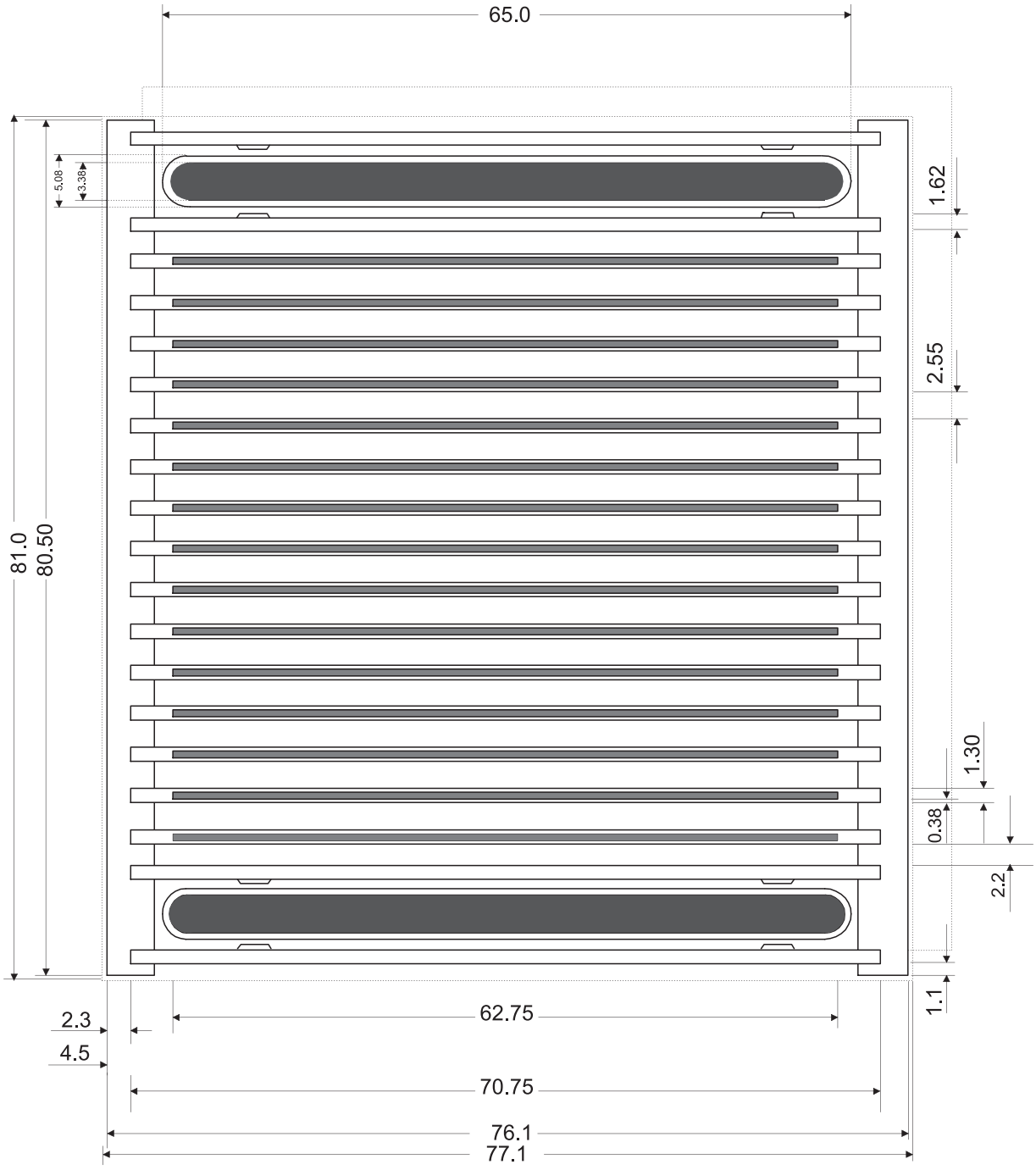

Fig. 4. Control fuel element (CE) of RSG GAS reactor (unit mm).

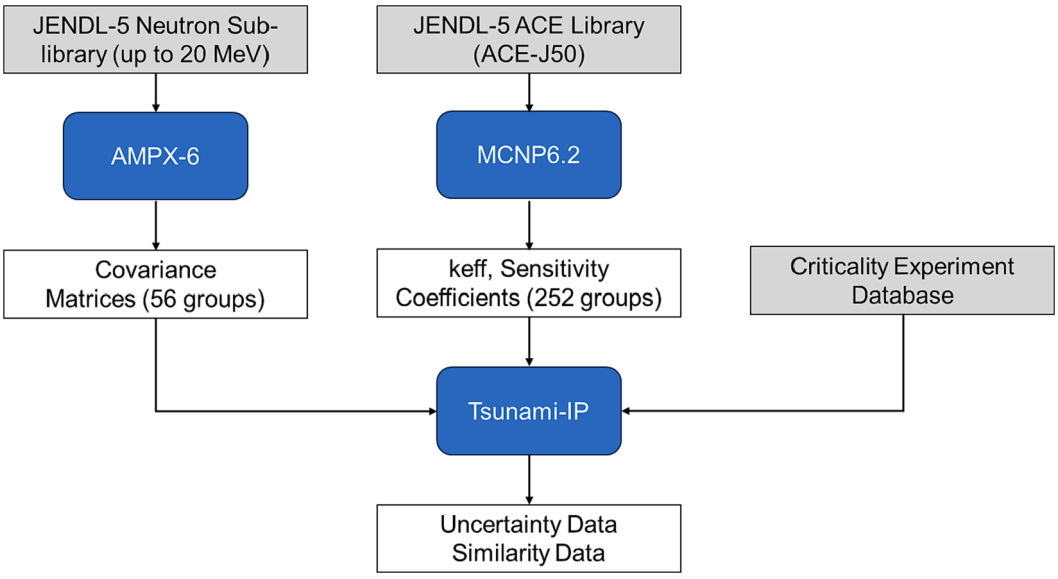

Fig. 5. Calculation flow of the sensitivity, uncertainty, and similarity analysis.

Table 3
Considered reaction types for the sensitivity coefficients (KSEN option).

No.	MCNP6.2 MT No.	Reaction Type
1	2	Elastic scattering
2	4	Inelastic scattering
3	–6	Fission
4	16	(n,2n) scattering
5	102	Capture (n,γ)
6	103	(n,p) proton production
7	104	(n,d) deuterium production
8	107	(n,α) alpha particle production
9	–7	Average number of neutrons produced per fission (total)
10	–1018	Fission spectrum

reactivity change from replacing the library is the summation of both S (α,β) thermal and fast library of hydrogen. Hence, in the study, the reactivity change of water is further broken down into H-1 and O-16 contributions. The contribution of H-1 is −162 pcm while the one of O-16 is + 96 pcm. Al-27 and Be-9 show negligible reactivity changes. Relatively strong absorber materials, i.e. Ag, In, and Cd, also do not show large reactivity changes. These results are also consistent with the ones obtained by Tada et al. (2023) mentioned above.

4.2. Sensitivity analysis

The sensitivity analysis has been conducted with the KSEN option of MCNP using JENDL-5, JENDL-4.0, and ENDF/B-VIII.0 libraries, for the selected case, i.e., Case 2-1 (Second group, 12 FEs, 6 CEs) where the full core was critical during C-8 regulation rod calibration. The sensitivity coefficients for each nuclide and nuclear reaction were obtained and sorted according to their absolute values. Furthermore, the sensitivity coefficients were grouped according to their signs into two groups as in our previous work (Liem et al. 2019a), one for sensitivity coefficients that tend to decrease keff (Table 6), and another one that tends to increase keff (Table 7). In the two tables, coefficients' absolute values smaller than 0.1 % were not shown, namely, only dominant coefficients were shown and discussed.

From Table 6, one can observe that the keff sensitivities in the decreasing direction were dominated by (n, gamma) reactions of H-1, U-235, Al-27, U-238, Be-9, Mn-55, Ag-109, In-115, Ag-107, Cd-113, and Fe-56. The (n, alpha) reactions of Be-9 and O-16, also contributed more weakly. As for the inter-library comparison, sensitivity coefficients differences compared to JENDL-5 of more than 5 % were observed for JENDL-4.0O-16 (n, alpha) reaction, and ENDF/B-VIII.0B-9 (n, gamma) reaction. One can expect that these differences originated from the corresponding cross section differences amongst the libraries.

From Table 7, one can observe that the sensitivities in the increasing direction were dominated (absolute values > 1.0 %) by U-235 (total nu) & (fission), H-1 (free gas, elastic) & (TSL, inelastic), Be-9 (elastic) & (n, 2n), O-16 (elastic), and Al-27 (elastic). As for the inter-library comparison, sensitivity coefficients differences compared to JENDL-5 of more than 5 % were observed for JENDL-4.0H-1 (free gas, elastic) & (TSL, inelastic), Be-9 (TSL, inelastic) & (TSL, elastic), ENDF/B-VIII.0 Al-27 (inelastic), U-238 (elastic) and Fe-56 (elastic).

The sensitivity analysis results of JENDL-5 showed similar trends as in our previous work of JENDL-4.0 (Liem et al., 2019a). The energy-dependent sensitivity profiles for some JENDL-5 dominant nuclide-reaction pairs are shown in Figs. 6 to 13. It can be observed that the use of 252 energy groups can catch the dominant resonance structures of the cross sections.

The U-235 sensitivity (Fig. 6) shows positive profiles for average ν and fission reactions, and a negative profile for (n,gamma) or capture reaction, in the thermal energy region (<1.0 eV). As for the U-238 sensitivity (Fig. 7), the negative profile of (n,gamma) reaction appears not only in the thermal energy region but at many resonance energies in the range of 1 eV to 1 keV. In the opposite direction of the resonances, the positive profile of elastic scattering can be observed. In the fast energy region of more than 1 MeV, several positive profiles fission related reactions, and inelastic reaction can be observed. The sensitivity of the free gas H-1 and bounded H-1 (Fig. 8) shows positive profiles in the free gas H-1 elastic scattering reaction (greater than 10 eV). In the thermal energy region, the bounded H-1 (TSL) inelastic scattering profile resembles the JENDL-4.0 where a sharp peak appears in the U-238 low energy resonance (6.67 eV). The free gas and bounded Be-9 sensitivity (Fig. 9) shows the dominant positive profile in the elastic scattering reaction, especially in the fast energy region. Fig. 10 indicates the mostly positive profile of O-16 elastic scattering reaction especially in the fast energy region. A relatively small negative profile of (n, alpha) reaction appears in the energy region of more than several MeV. The Al-27 sensitivity (Fig. 11) shows a large negative profile of capture reaction in the thermal energy region (below 1 eV), while relatively smaller positive profiles for elastic and inelastic scattering reactions appear in the fast energy region. The Fe-56 sensitivity (Fig. 12) shows two dominant profiles, namely, a positive elastic scattering profile and a negative

Table 4
JENDL-5 nuclides with covariance data processed by AMPX code.

No.	Nuclide ID	ZAID	File Name	No.	Nuclide ID	ZAID	File Name
1	125	1001	n_001-H-001.dat	56	9349	93,238	n_093-Np-238.dat
2	525	5010	n_005-B-010.dat	57	9352	93,239	n_093-Np-239.dat
3	528	5011	n_005-B-011.dat	58	9428	94,236	n_094-Pu-236.dat
4	628	6013	n_006-C-013.dat	59	9431	94,237	n_094-Pu-237.dat
5	725	7014	n_007-N-014.dat	60	9434	94,238	n_094-Pu-238.dat
6	728	7015	n_007-N-015.dat	61	9437	94,239	n_094-Pu-239.dat
7	825	8016	n_008-O-016.dat	62	9440	94,240	n_094-Pu-240.dat
8	1125	11,023	n_011-Na-023.dat	63	9443	94,241	n_094-Pu-241.dat
9	1725	17,035	n_017-Cl-035.dat	64	9446	94,242	n_094-Pu-242.dat
10	2231	22,048	n_022-Ti-048.dat	65	9452	94,244	n_094-Pu-244.dat
11	2425	24,050	n_024-Cr-050.dat	66	9458	94,246	n_094-Pu-246.dat
12	2431	24,052	n_024-Cr-052.dat	67	9540	95,240	n_095-Am-240.dat
13	2434	24,053	n_024-Cr-053.dat	68	9543	95,241	n_095-Am-241.dat
14	2437	24,054	n_024-Cr-054.dat	69	9546	95,242	n_095-Am-242.dat
15	2525	25,055	n_025-Mn-055.dat	70	9547	95,242	n_095-Am-242 m1.dat
16	2631	26,056	n_026-Fe-056.dat	71	9549	95,243	n_095-Am-243.dat
17	2637	26,058	n_026-Fe-058.dat	72	9552	95,244	n_095-Am-244.dat
18	2725	27,059	n_027-Co-059.dat	73	9553	95,244	n_095-Am-244 m1.dat
19	2825	28,058	n_028-Ni-058.dat	74	9625	96,240	n_096-Cm-240.dat
20	2831	28,060	n_028-Ni-060.dat	75	9628	96,241	n_096-Cm-241.dat
21	4025	40,090	n_040-Zr-090.dat	76	9631	96,242	n_096-Cm-242.dat
22	8225	82,204	n_082-Pb-204.dat	77	9634	96,243	n_096-Cm-243.dat
23	8231	82,206	n_082-Pb-206.dat	78	9637	96,244	n_096-Cm-244.dat
24	8234	82,207	n_082-Pb-207.dat	79	9640	96,245	n_096-Cm-245.dat
25	8237	82,208	n_082-Pb-208.dat	80	9643	96,246	n_096-Cm-246.dat
26	8325	83,209	n_083-Bi-209.dat	81	9646	96,247	n_096-Cm-247.dat
27	8925	89,225	n_089-Ac-225.dat	82	9649	96,248	n_096-Cm-248.dat
28	8928	89,226	n_089-Ac-226.dat	83	9652	96,249	n_096-Cm-249.dat
29	8931	89,227	n_089-Ac-227.dat	84	9655	96,250	n_096-Cm-250.dat
30	9025	90,227	n_090-Th-227.dat	85	9740	97,245	n_097-Bk-245.dat
31	9028	90,228	n_090-Th-228.dat	86	9743	97,246	n_097-Bk-246.dat
32	9031	90,229	n_090-Th-229.dat	87	9746	97,247	n_097-Bk-247.dat
33	9034	90,230	n_090-Th-230.dat	88	9749	97,248	n_097-Bk-248.dat
34	9037	90,231	n_090-Th-231.dat	89	9752	97,249	n_097-Bk-249.dat
35	9040	90,232	n_090-Th-232.dat	90	9755	97,250	n_097-Bk-250.dat
36	9043	90,233	n_090-Th-233.dat	91	9843	98,246	n_098-Cf-246.dat
37	9046	90,234	n_090-Th-234.dat	92	9849	98,248	n_098-Cf-248.dat
38	9125	91,229	n_091-Pa-229.dat	93	9852	98,249	n_098-Cf-249.dat
39	9128	91,230	n_091-Pa-230.dat	94	9855	98,250	n_098-Cf-250.dat
40	9131	91,231	n_091-Pa-231.dat	95	9858	98,251	n_098-Cf-251.dat
41	9134	91,232	n_091-Pa-232.dat	96	9861	98,252	n_098-Cf-252.dat
42	9137	91,233	n_091-Pa-233.dat	97	9864	98,253	n_098-Cf-253.dat
43	9213	92,230	n_092-U-230.dat	98	9867	98,254	n_098-Cf-254.dat
44	9216	92,231	n_092-U-231.dat	99	9911	99,251	n_099-Es-251.dat
45	9219	92,232	n_092-U-232.dat	100	9912	99,252	n_099-Es-252.dat
46	9222	92,233	n_092-U-233.dat	101	9913	99,253	n_099-Es-253.dat
47	9225	92,234	n_092-U-234.dat	102	9914	99,254	n_099-Es-254.dat
48	9228	92,235	n_092-U-235.dat	103	9915	99,254	n_099-Es-254 m1.dat
49	9231	92,236	n_092-U-236.dat	104	9916	99,255	n_099-Es-255.dat
50	9234	92,237	n_092-U-237.dat	105	9936	100,255	n_100-Fm-255.dat
51	9237	92,238	n_092-U-238.dat				
52	9337	93,234	n_093-Np-234.dat				
53	9340	93,235	n_093-Np-235.dat				
54	9343	93,236	n_093-Np-236.dat				
55	9346	93,237	n_093-Np-237.dat				

Table 5
Criticality analysis results (keff).

Case	First criticality and excess reactivity loading(First Group)	JENDL-5			JENDL-4.0			ENDF/B-VIII.0		
1-1	First criticality (9 FEs, 6 CEs, RR = 475 mm)	1.00801	±	0.00008	1.00477	±	0.00008	1.00547	±	0.00008
1-2	Full core (12 FEs, 6 CEs, CRs all up)	1.10167	±	0.00008	1.09949	±	0.00008	1.09912	±	0.00007
1-3	Full core (12 FEs, 6 CEs, CRs all down)	0.92088	±	0.00008	0.91957	±	0.00008	0.91974	±	0.00008
Case	Calibrated rod/grid position (calibrated rod position/other rod bank position)(Second Group, 12 FEs, 6 CEs)	JENDL-5			JENDL-4.0			ENDF/B-VIII.0		
2-1	JDA06 / C-8 (600 mm / 290 mm)	1.00465	±	0.00008	1.00282	±	0.00008	1.00302	±	0.00008
2-2	JDA01 / E-9 (600 mm / 284 mm)	1.00478	±	0.00008	1.00257	±	0.00008	1.00301	±	0.00008
2-3	JDA03 / F-8 (600 mm / 293 mm)	1.00599	±	0.00008	1.00379	±	0.00008	1.00406	±	0.00008
2-4	JDA05 / C-5 (600 mm / 288 mm)	1.00584	±	0.00008	1.00400	±	0.00008	1.00415	±	0.00008
2-5	JDA04 / F-5 (600 mm / 290 mm)	1.00650	±	0.00008	1.00431	±	0.00008	1.00452	±	0.00008
2-6	JDA07 / D-4 (600 mm / 282 mm)	1.00614	±	0.00008	1.00422	±	0.00008	1.00426	±	0.00008

Table 6
Sensitivities of keff in the decreasing direction (abs. value > 0.1 %).

Nuclide	Reaction	Sensitivity and Ratio between Libraries				
		JENDL-5.0	JENDL-4.0	J4/J5	ENDF/B-VIII.0	E8/J5
H-1	n,gamma	-1.68E-01	-1.70E-01	1.01	-1.67E-01	1.00
U-235	n,gamma	-1.23E-01	-1.22E-01	0.99	-1.24E-01	1.00
Al-27	n,gamma	-4.87E-02	-4.93E-02	1.01	-5.00E-02	1.03
U-238	n,gamma	-3.77E-02	-3.80E-02	1.01	-3.76E-02	1.00
Be-9	n,gamma	-4.74E-03	-4.79E-03	1.01	-5.37E-03	1.13
Mn-55	n,gamma	-4.39E-03	-4.42E-03	1.01	-4.36E-03	0.99
Ag-109	n,gamma	-3.63E-03	-3.64E-03	1.00	-3.58E-03	0.98
Be-9	n,alpha	-2.93E-03	-3.00E-03	1.03	-3.02E-03	1.03
In-115	n,gamma	-2.52E-03	-2.54E-03	1.01	-2.53E-03	1.00
Ag-107	n,gamma	-1.92E-03	-1.92E-03	1.00	-1.88E-03	0.98
O-16	n,alpha	-1.64E-03	-1.22E-03	0.75	-1.71E-03	1.05
Cd-113	n,gamma	-1.45E-03	-1.40E-03	0.96	-1.43E-03	0.98
Fe-56	n,gamma	-1.22E-03	-1.24E-03	1.01	-1.23E-03	1.01

(shaded figures show a discrepancy of more than 5 %).

capture profile. The elastic scattering profile has a large profile in the thermal energy region and complicated profiles stem from the resonances. The capture profile is much simpler which shows a large negative profile in the thermal energy region (below 1 eV). The less dominant (n,gamma) or capture sensitivity profiles of Mn, Ag, In, and Cd isotopes are shown in Fig. 13. Among the isotopes, the Mn-55 shows a notably large negative profile in the thermal energy region (below 1 eV).

4.3. Uncertainty analysis

The uncertainty analysis has been conducted with TSUNAMI-IP using JENDL-5 and ENDF/B-VIII.0 libraries, for the selected case, i.e., Case 2-1 (Second group, 12 FEs, 6 CEs) where the full core was critical during C-8 regulation rod calibration. The uncertainty analysis results are shown in Table 8 while the uncertainty main contributors (for JENDL-5) are shown in Table 9.

From Table 8, the keff uncertainties due to nuclear data are presented for three combinations of sensitivity coefficients and covariance matrices, i.e. JENDL-5 only, JENDL-5 & ENDF/B-VIII.0, and ENDF/B-VIII.0. If only 105 covariance matrices of JENDL-5 was used the uncertainty was around 620 pcm, while if the additional covariance matrices of ENDF/B-VIII.0 was also used, the uncertainty increased to 644 pcm, hence, for the present system, the difference was small, i.e., around 24 pcm. The uncertainty of ENDF/B-VIII.0 was evaluated to be

Table 7
Sensitivities of keff in the increasing direction (abs. value > 0.1 %).

Nuclide	Reaction	Sensitivity and Ratio between Libraries				
		JENDL-5.0	JENDL-4.0	J4/J5	ENDF/B-VIII.0	E8/J5
U-235	total nu	9.95E-01	9.95E-01	1.00	9.95E-01	1.00
U-235	fission	3.51E-01	3.50E-01	1.00	3.51E-01	1.00
H-1	elastic	2.67E-01	2.90E-01	1.08	2.68E-01	1.00
Be-9	elastic	5.85E-02	6.01E-02	1.03	5.94E-02	1.02
H-1 (TSL)	inelastic	4.80E-02	2.83E-02	0.59	4.90E-02	1.02
O-16	elastic	4.31E-02	4.48E-02	1.04	4.33E-02	1.01
Al-27	elastic	2.71E-02	2.75E-02	1.02	2.77E-02	1.02
Be-9	n,2n	1.11E-02	1.14E-02	1.03	1.09E-02	0.99
Al-27	inelastic	9.66E-03	9.98E-03	1.03	1.08E-02	1.12
Be-9 (TSL)	inelastic	5.17E-03	4.40E-03	0.85	4.88E-03	0.94
U-238	total nu	4.90E-03	5.00E-03	1.02	4.70E-03	0.96
U-238	elastic	4.84E-03	4.61E-03	0.95	4.46E-03	0.92
Be-9 (TSL)	elastic	3.82E-03	3.49E-03	0.91	3.61E-03	0.95
U-238	fission	3.34E-03	3.42E-03	1.02	3.33E-03	1.00
U-238	inelastic	2.21E-03	2.17E-03	0.98	2.16E-03	0.98
Fe-56	elastic	1.83E-03	1.84E-03	1.01	1.94E-03	1.07

TSL: Thermal Scattering Law; (shaded figures show a discrepancy of more than 5 %).

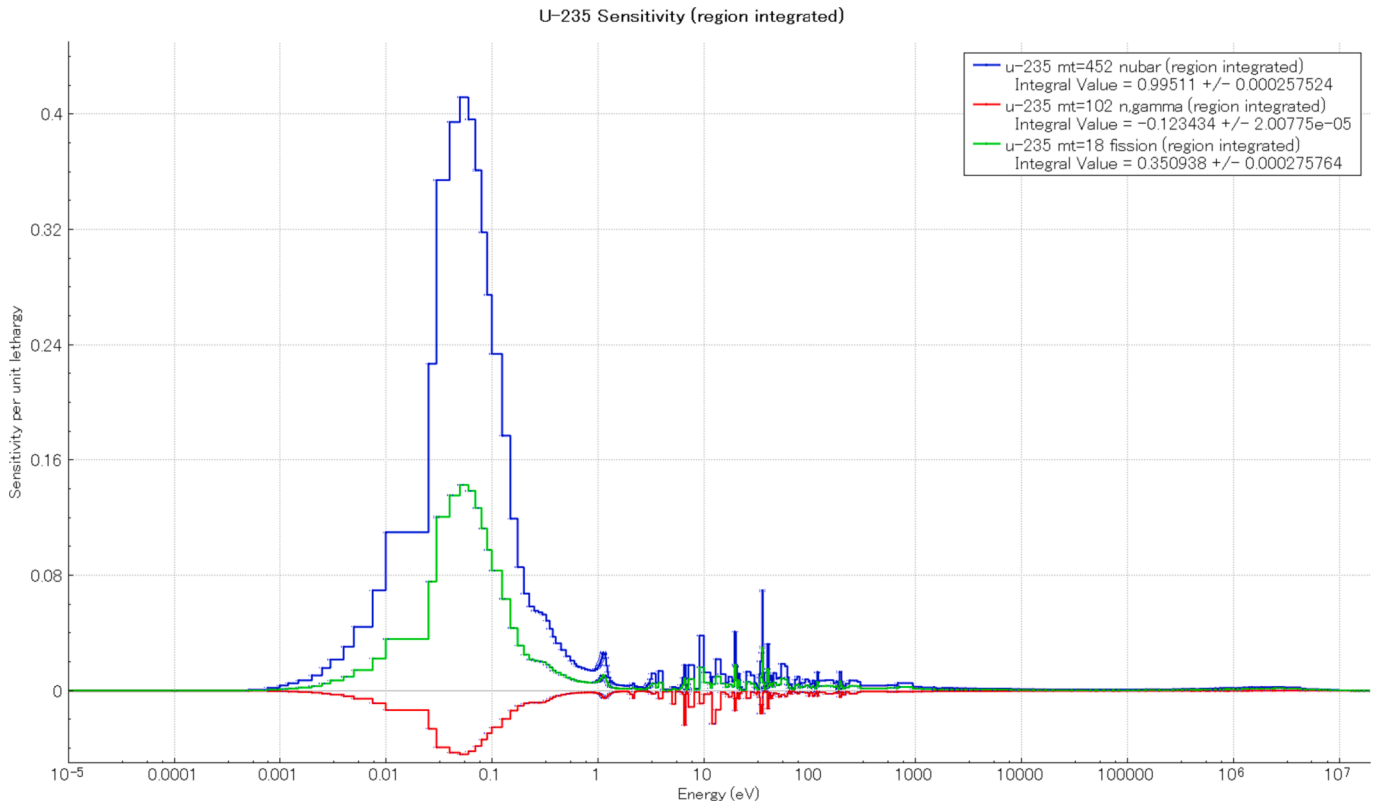

Fig. 6. Energy-dependent sensitivities of k to U-235 cross-sections (JENDL-5).

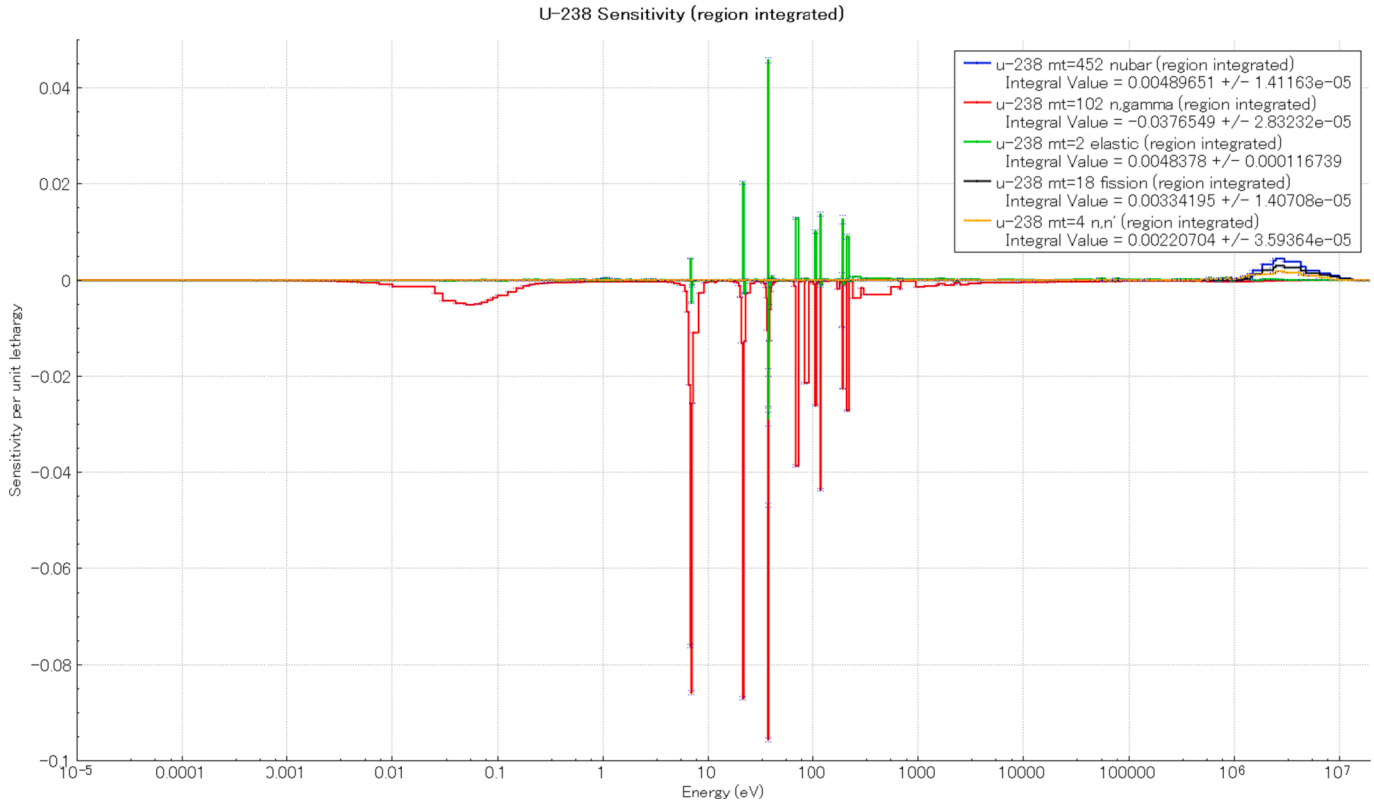

Fig. 7. Energy-dependent sensitivities of k to U-238 cross-sections (JENDL-5).

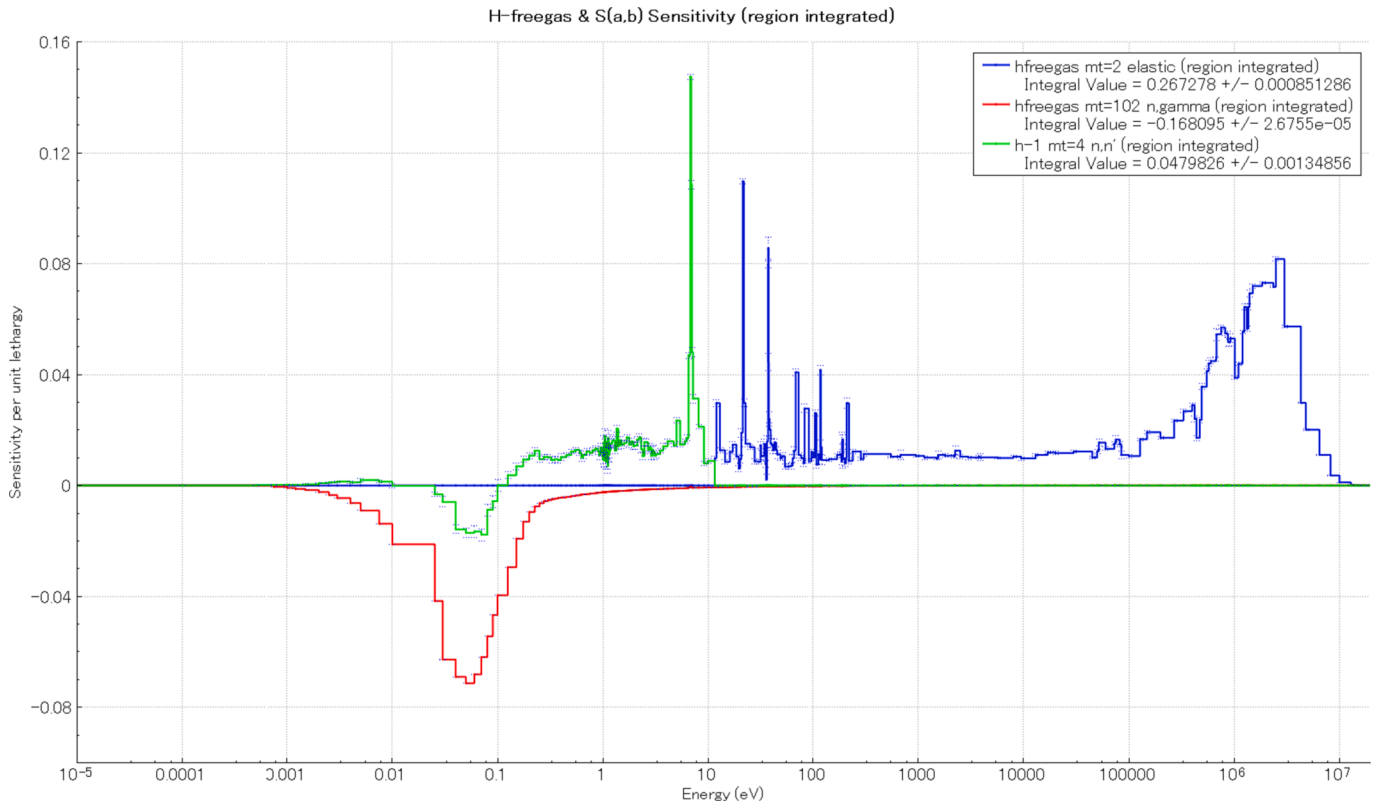

Fig. 8. Energy-dependent sensitivities of k to H-1 free-gas and S(α,β) cross-sections (JENDL-5).

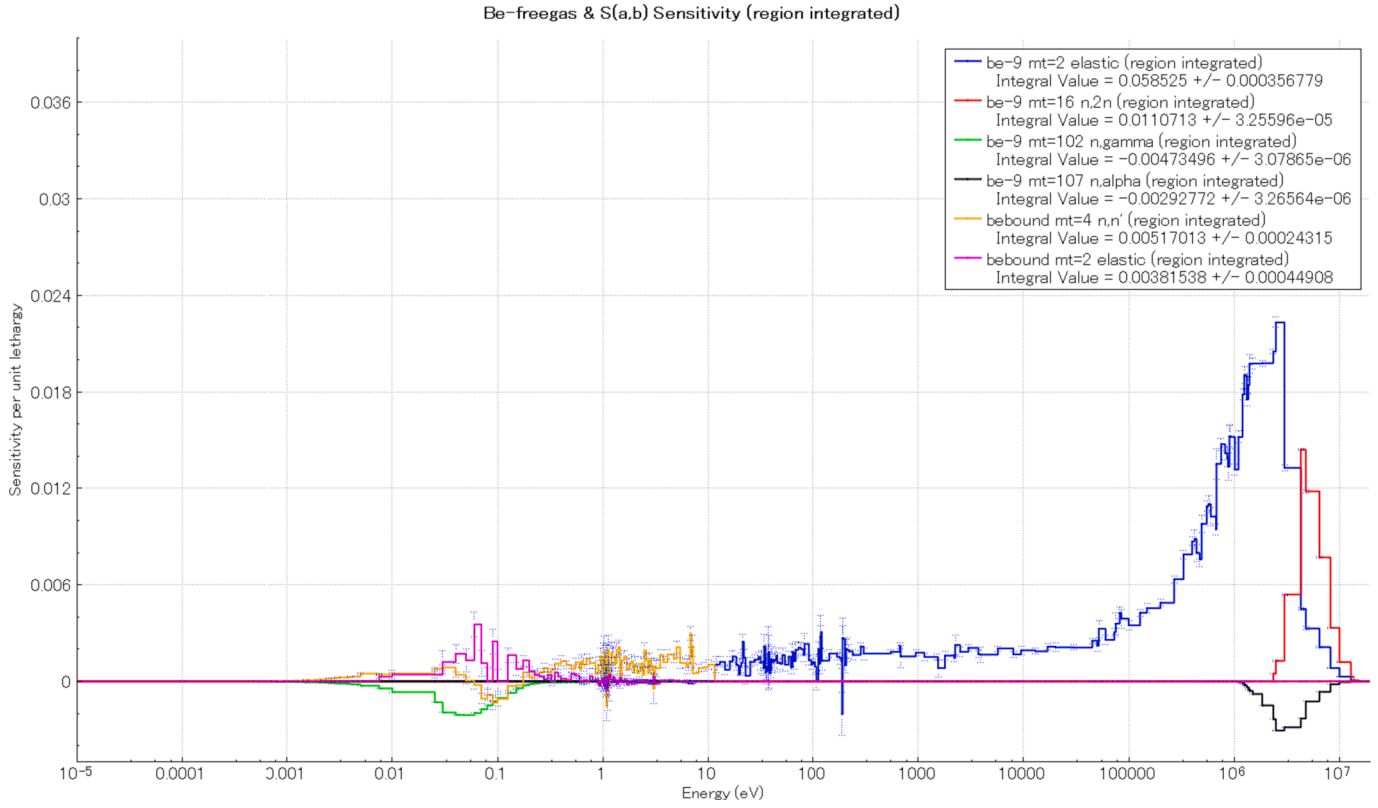

Fig. 9. Energy-dependent sensitivities of k to Be-9 free-gas and S(α,β) cross-sections (JENDL-5).

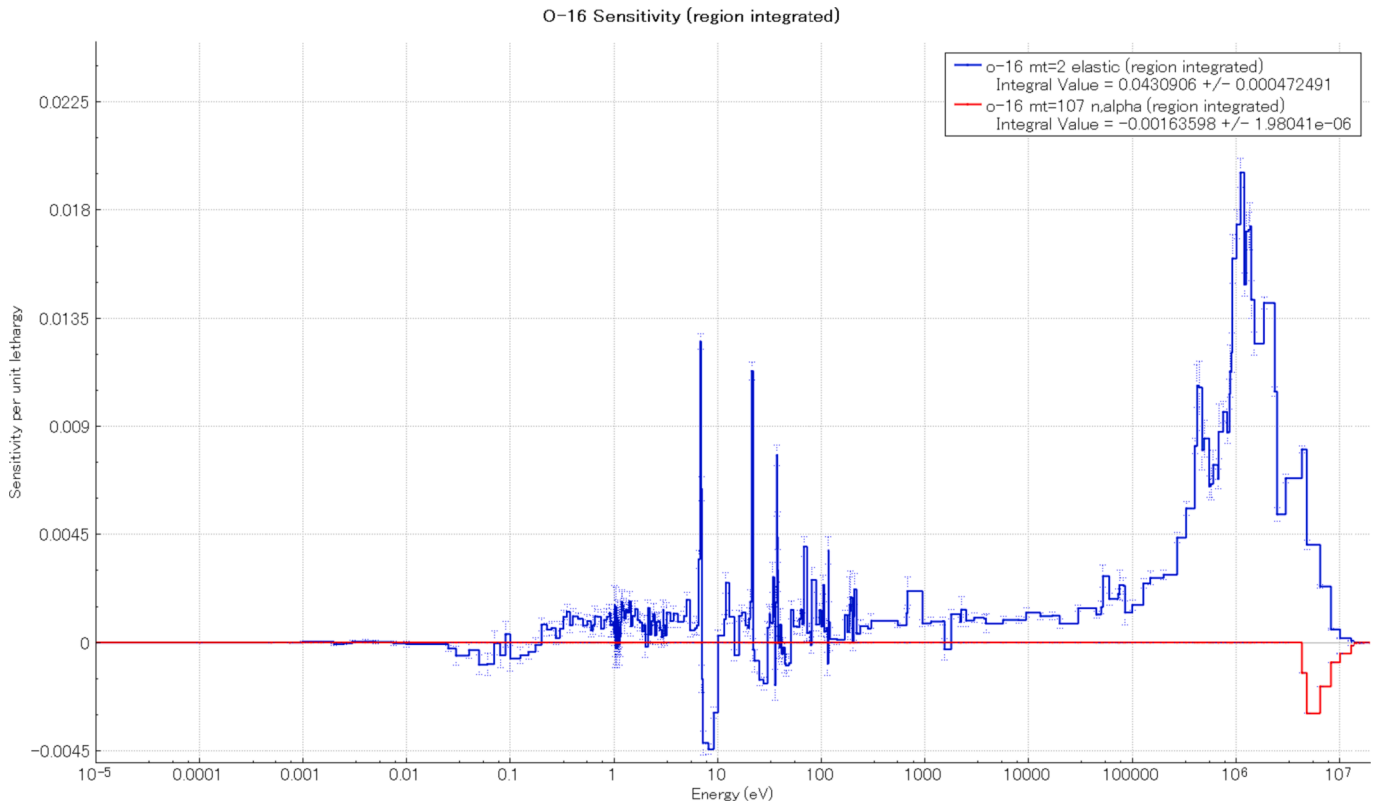

Fig. 10. Energy-dependent sensitivities of k to O-16 cross-sections (JENDL-5).

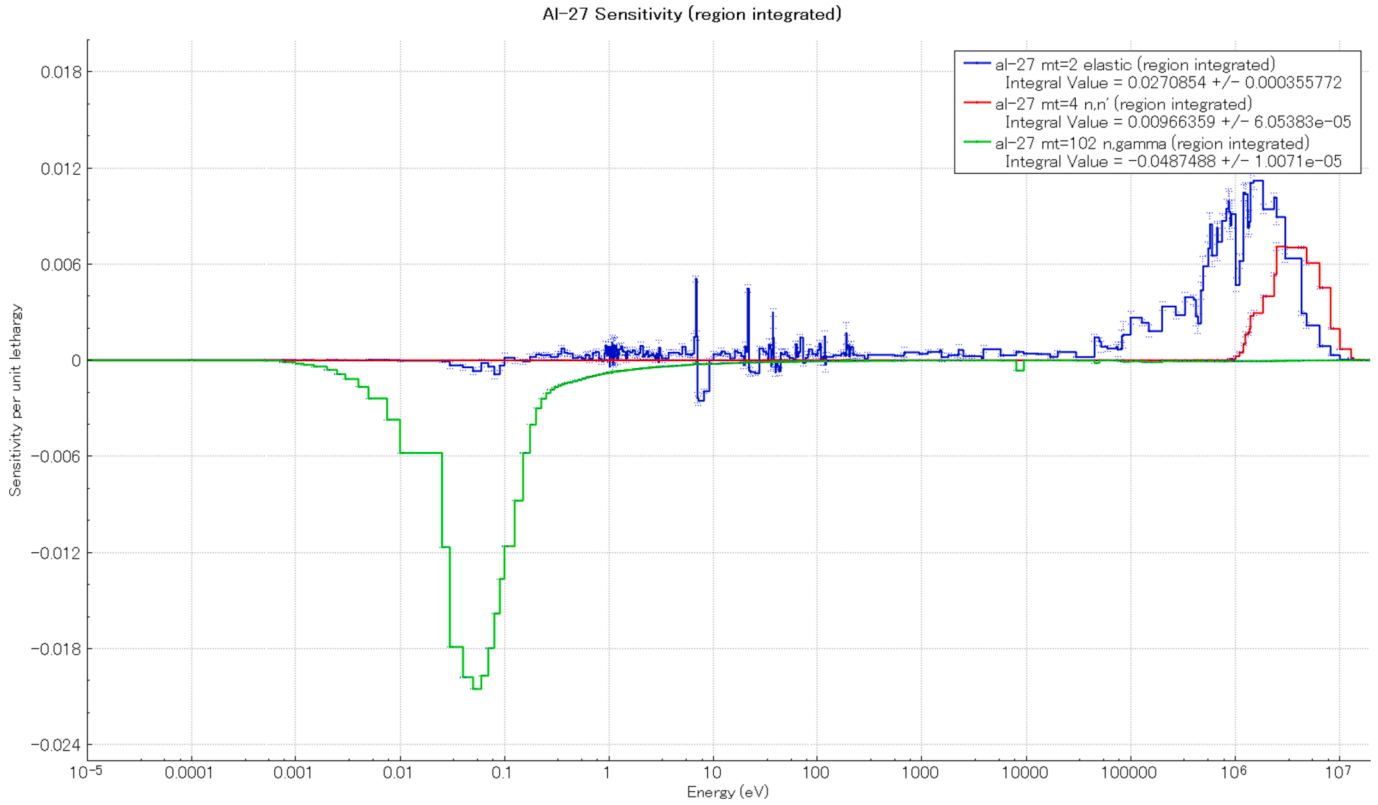

Fig. 11. Energy-dependent sensitivities of k to Al-27 cross-sections (JENDL-5).

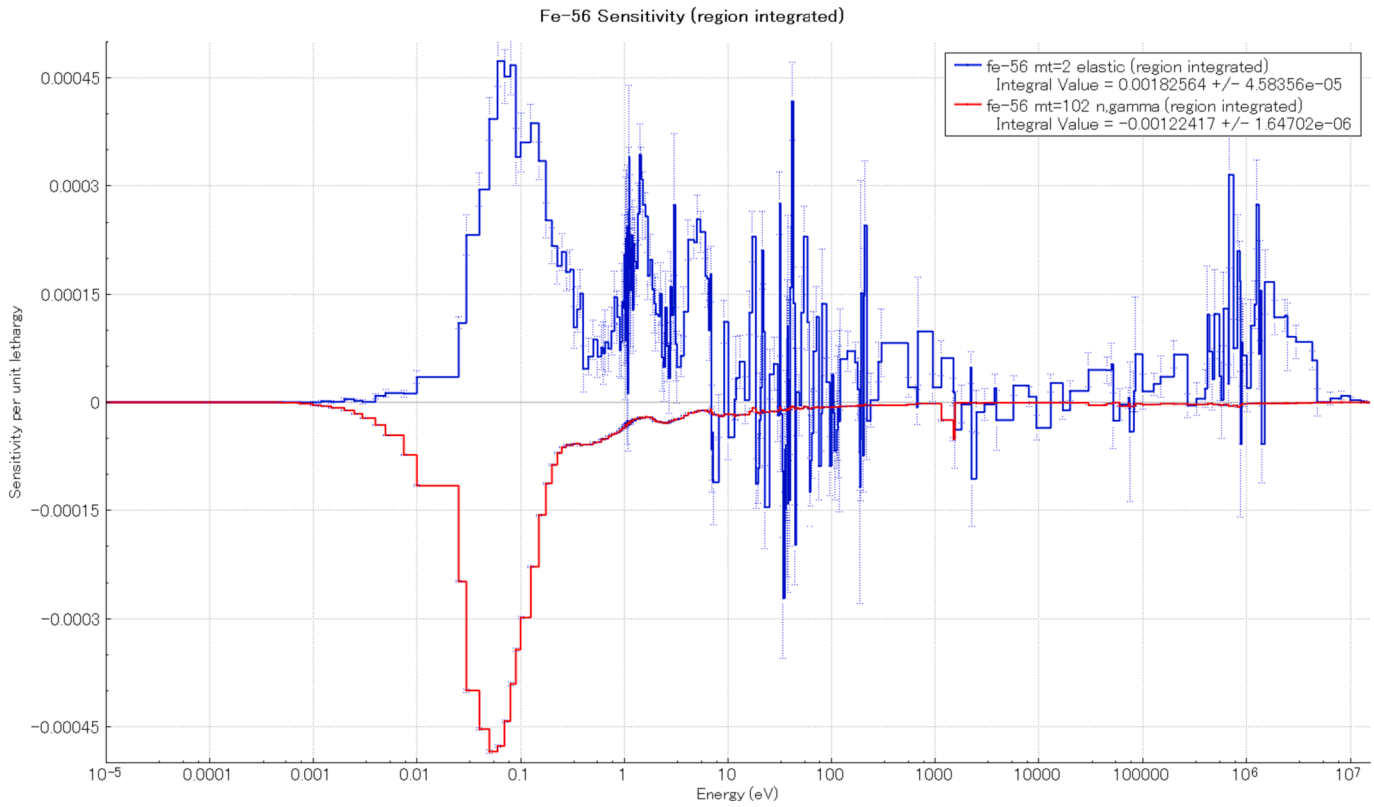

Fig. 12. Energy-dependent sensitivities of k to Fe-56 cross-sections (JENDL-5).

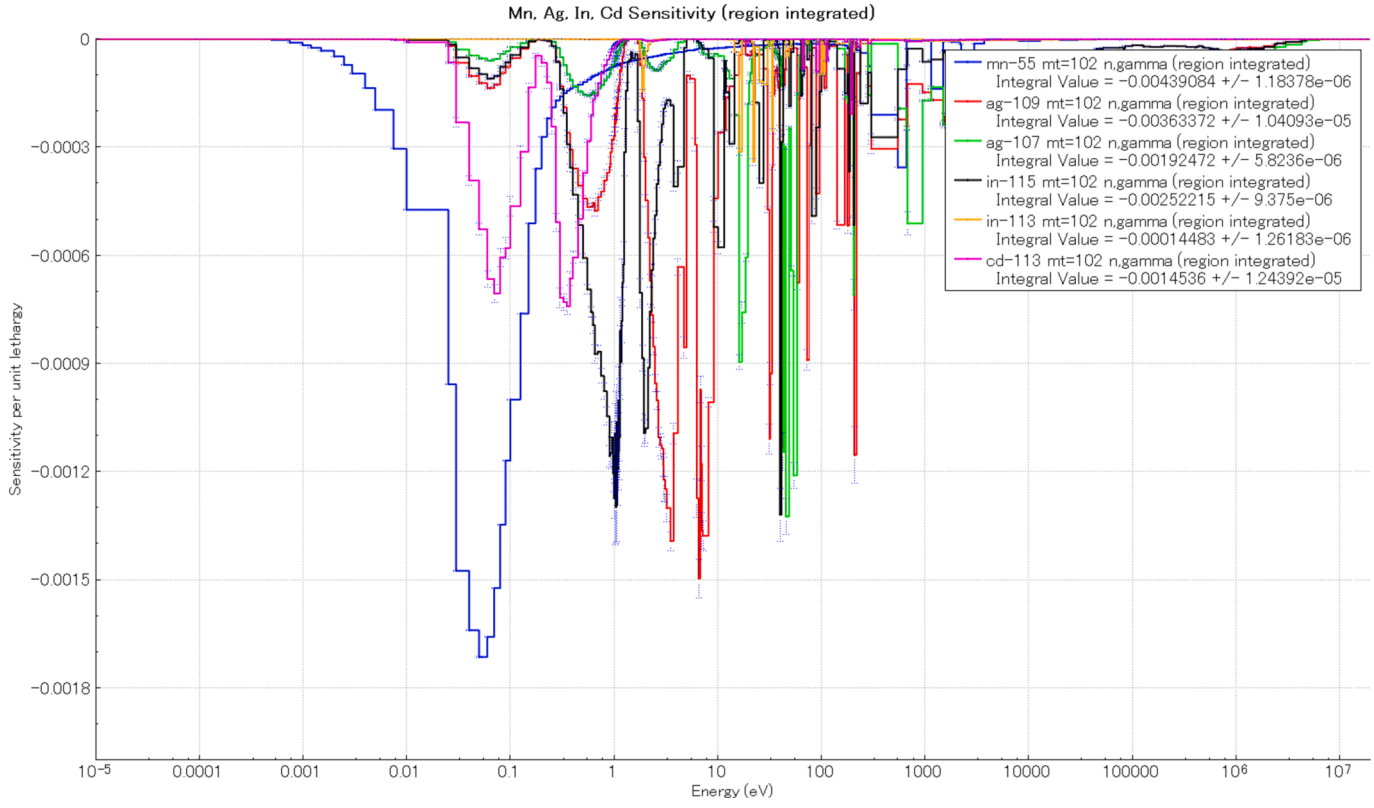

Fig. 13. Energy-dependent sensitivities of k to Mn, Ag, In and Cd isotopes cross-sections (JENDL-5).

Table 8
Uncertainty analysis results (pcm = 10^{-5}).

Sensitivity Coefficients	Covariance Matrices	Uncertainty (pcm)
JENDL-5 (MCNP6.2, KSEN option)	JENDL-5 only (AMPX-6)	620
JENDL-5 (MCNP6.2, KSEN option)	JENDL-5 & ENDF/B-VIII.0 * (AMPX-6)	644
ENDF/B-VIII.0 (MCNP6.2, KSEN option)	ENDF/B-VIII.0 (SCALE 6.3.0)	637

*: For JENDL-5 nuclides which have no covariance data.

637 pcm, which was comparable with the ones of the JENDL-5. In other words, the nuclear data uncertainties of JENDL-5 and ENDF/B-VIII.0 are in the same order.

In Table 9, the JENDL-5 uncertainty contributors are sorted and listed when the JENDL-5 & ENDF/B-VIII.0 covariance matrices were used. The dominant contributors of the table, i.e. > 0.1 %, are U-235 (chi), (nubar) & (fission), H-1 (n, gamma), (elastic) & (TSL, inelastic), O-16 (elastic), and Al-27 (n, gamma). In the RSG GAS, the LEU (19.75 wt% U-235 enrichment) is used and consequently, the U-235 fission-related parameters contribute to the keff uncertainty significantly. Water is used as a moderator and coolant material so that it exists in the core, reflector, and other structural regions in large quantities. The H-1 component of the water contributes significantly both as free gas (elastic) and when bounded by O-16 (TSL, inelastic).

Recalling back the JENDL-5 [C/E-1] of Case 2-1 shown in Table 5 (~465 pcm), the evaluated keff uncertainty of JENDL-5 of 644 pcm was comparable. However, it is premature to conclude that the deviation of [C/E] from 1.0 originated only from the nuclear data, since other uncertainties were not taken into account, such as uncertainties in the compositions, dimensions, criticality measurements, etc.

4.4. Similarity analysis

The similarity analysis results are shown in Tables 10 and 11. In Table 10, the criticality experiment series whose member cases have $c_k > 0.8$ are tabulated. We found that 16 criticality experiment series under the thermal spectrum category with various numbers of member cases show $c_k > 0.8$, and their total cases are 125 experiments. Surprisingly, amongst the 16 series, 14 of them related to high-enriched uranium (HEU) although the RSG GAS core uses a relatively low 19.75 wt% enrichment (LEU). The other 2 series are under the LEU group. Amongst these 125 experiments, the top 20 cases are listed in Table 11. The largest c_k (0.857) was found for HEU-MISC-THERM-001-023. HEU-MISC-THERM-001 is a criticality experiment series conducted by ORNL with the SPERT-D experimental reactor (Crawford and Palmer, 1992). In the SPERT-D experiment series, aluminum-clad plate-type fuel in water, dilute uranyl nitrate, or borated uranyl nitrate was used. Except that SPERT-D used HEU (93 wt% enrichment), the fuel elements are indeed very similar to the ones of the RSG GAS.

From Table 11, it can be concluded that at present there is no single criticality experiment that has a strong similarity (in this case $c_k > 0.9$) with the RSG GAS core. Therefore, it is suggested that more criticality benchmark experiments similar to RSG GAS should be conducted in the future. Furthermore, the RSG GAS first criticality experiments should be considered to be included in the benchmark databases.

Table 10
Similarity analysis results with $c_k > 0.8$.

No.	Experiment Series	Cases
1	HEU-COMP-THERM-010	1
2	HEU-COMP-THERM-021	41
3	HEU-MET-THERM-006	12
4	HEU-MISC-THERM-002	1
5	HEU-MISC-THERM-001	5
6	HEU-MISC-THERM-002	1
7	HEU-SOL-THERM-005	11
8	HEU-SOL-THERM-006	21
9	HEU-SOL-THERM-007	7
10	HEU-SOL-THERM-021	1
11	HEU-SOL-THERM-031	2
12	HEU-SOL-THERM-036	3
13	HEU-SOL-THERM-044	13
14	HEU-SOL-THERM-048	1
15	LEU-SOL-THERM-006	4
16	LEU-SOL-THERM-016	1
	Total number of cases	**125**

Table 9
Uncertainty contributors (>0.001 %).

Nuclide	Reaction	with	Nuclide	Reaction	% dR/R due to this matrix		
u-235	chi	with	u-235	chi	3.76E-01	+/−	1.78E-04
hfreegas	n,gamma	with	hfreegas	n,gamma	3.48E-01	+/−	9.93E-06
u-235	nubar	with	u-235	nubar	3.00E-01	+/−	1.19E-05
h-1	n,n'	with	h-1	n,n'	2.41E-01	+/−	6.47E-04
u-235	fission	with	u-235	fission	1.62E-01	+/−	1.08E-05
hfreegas	elastic	with	hfreegas	elastic	1.27E-01	+/−	2.85E-05
hfreegas	elastic	with	hfreegas	n,gamma	−1.14E-01	+/−	1.92E-05
al-27	n,gamma	with	al-27	n,gamma	1.07E-01	+/−	8.73E-07
al-27	elastic	with	al-27	elastic	8.63E-02	+/−	7.24E-05
al-27	n,n'	with	al-27	n,n'	7.15E-02	+/−	2.28E-05
be-9	elastic	with	be-9	elastic	6.29E-02	+/−	1.17E-05
be-9	n,2*n*	with	be-9	n,2*n*	3.56E-02	+/−	8.63E-06
u-238	n,gamma	with	u-238	n,gamma	3.46E-02	+/−	5.28E-07
u-235	n,gamma	with	u-235	n,gamma	3.19E-02	+/−	1.48E-07
u-235	fission	with	u-235	n,gamma	−2.80E-02	+/−	4.38E-07
be-9	n,gamma	with	be-9	n,gamma	2.37E-02	+/−	2.01E-07
u-238	n,n'	with	u-238	n,n'	2.03E-02	+/−	6.28E-06
bebound	n,n'	with	bebound	n,n'	1.86E-02	+/−	1.27E-05
be-9	n,2*n*	with	be-9	elastic	−1.71E-02	+/−	1.82E-06
be-9	n,alpha	with	be-9	n,alpha	1.43E-02	+/−	1.77E-07
fe-56	n,gamma	with	fe-56	n,gamma	1.37E-02	+/−	1.17E-07
o-16	elastic	with	o-16	elastic	1.28E-02	+/−	7.51E-07
u-238	elastic	with	u-238	elastic	1.26E-02	+/−	2.76E-06
ag-109	n,gamma	with	ag-109	n,gamma	1.20E-02	+/−	1.81E-07
u-238	elastic	with	u-238	n,gamma	1.16E-02	+/−	2.00E-06

Table 11
Top-20 experiments with $c_k > 0.8$.

No	Experiment Case	keff	keff (SD)	Uncertainty (%)	c_k
1	HEU-MISC-THERM-001-023	1.0037	0.0003	0.7085	0.857
2	HEU-MISC-THERM-001-022	1.0011	0.0003	0.7323	0.856
3	HEU-MISC-THERM-001-021	1.0014	0.0003	0.7753	0.849
4	HEU-MET-THERM-006-018	0.9983	0.0003	0.7756	0.848
5	HEU-MISC-THERM-001-020	0.9984	0.0003	0.8173	0.843
6	HEU-MET-THERM-006-017	0.9978	0.0003	0.8326	0.839
7	HEU-MET-THERM-006-013	1.0206	0.0003	0.9142	0.830
8	HEU-MET-THERM-006-016	1.0017	0.0003	0.8206	0.829
9	HEU-SOL-THERM-006-015	1.0070	0.0002	0.6192	0.828
10	HEU-SOL-THERM-006-024	1.0081	0.0002	0.6155	0.828
11	HEU-SOL-THERM-006-019	1.0072	0.0003	0.6117	0.828
12	HEU-SOL-THERM-006-005	1.0082	0.0002	0.6242	0.827
13	HEU-MET-THERM-006-010	1.0076	0.0003	0.9545	0.826
14	HEU-SOL-THERM-005-004	1.0093	0.0003	0.6764	0.825
15	HEU-MET-THERM-006-011	0.9994	0.0003	0.9023	0.825
16	HEU-SOL-THERM-006-006	0.9994	0.0002	0.5799	0.824
17	HEU-MET-THERM-006-002	0.9993	0.0003	0.9626	0.824
18	HEU-SOL-THERM-006-016	0.9989	0.0002	0.5755	0.824
19	HEU-MET-THERM-006-003	1.0041	0.0003	0.9198	0.824
20	HEU-SOL-THERM-044-024	1.0200	0.0005	0.6459	0.823

SD: Standard Deviation

5. Concluding remarks

The JENDL-5 criticality, sensitivity, uncertainty, and similarity analyses were conducted for the clean first core of the RSG GAS Multipurpose Reactor, which is a beryllium-reflected, light-water moderated, 19.75 wt% enriched LEU-fueled MTR. The sensitivity coefficients needed were prepared with the KSEN option of MCNP6.2 for JENDL-5, JENDL-4.0, and ENDF/B-VIII.0. New covariance matrices were prepared with AMPX-6 for JENDL-5 only and the combined JENDL-5 & ENDF/B-VIII.0 for JENDL-5 nuclides with missing covariance data. The nuclear data-originated uncertainty was finally estimated with the TSUNAMI-IP module of SCALE-6.2.

The criticality (keff) analysis results ([C/E-1]) showed a maximum overestimation of 801 pcm, 477 pcm, and 547 pcm, for JENDL-5, JENDL-4.0 and ENDF/B-VIII.0, respectively. Dominant nuclide-reaction sensitivities and several large differences between libraries were identified. The keff uncertainty originated from the nuclear data was estimated to be 620 pcm, 644 pcm, and 637 pcm for JENDL-5 only, JENDL-5 & ENDF/B-VIII.0, and ENDF/B-VIII.0 covariance data, respectively, which are comparable with the keff ([C/E-1]) values.

The similarity analysis results showed that at present there is no single criticality experiment that has a strong similarity ($c_k > 0.9$) with the RSG GAS core.

CRediT authorship contribution statement

Peng Hong Liem: Conceptualization, Methodology, Investigation, Formal analysis, Data curation, Visualization, Writing – original draft, Writing – review & editing, Supervision. **Donny Hartanto:** Data curation, Formal analysis, Methodology, Software, Visualization, Writing – original draft, Writing – review & editing.

Declaration of competing interest

The authors declare that they have no known competing financial interests or personal relationships that could have appeared to influence the work reported in this paper.

Data availability

The authors do not have permission to share data.

Acknowledgments

We express our gratitude to all members of the commissioning group of RSG GAS for their efforts in compiling the criticality experiment data. We are also grateful to Mrs. Suzuko Ikegami for the preparation of the tables and graphs.

References

BATAN, 1980. Multipurpose Reactor G. A. Siwabessy Safety Analysis Report - Rev. 7, Jakarta.

Bostelmann, F., et al., 2021. On the creation of the new ENDF/B-VIII.0 Covariance Library for SCALE Applications with AMPX. In: Proceedings of International Conference on Mathematics and Computational Methods Applied to Nuclear Science and Engineering (M&C 2021), Raleigh, North Carolina, United States, October 3-7.

Brown, D.A., et al., 2018. ENDF/B-VIII.0: the 8-th Major Release of the nuclear reaction data library with CIELO-Project Cross Sections, New Standards and Thermal Scattering Data. Nucl. Data Sheets 148 (2018), 1–42.

Chadwick, M.B., et al., 2011. ENDF/B-VII.1 nuclear data for science and technology: cross-sections, covariances, fission product yields and decay data. Nucl. Data Sheets 112 (12), 2887–2996.

Crawford, C., Palmer, B., 1992. Validation of MCNP: SPERT-D and BORAX-V fuel. Technical Report WINCO-1112, Westinghouse Idaho Nuclear Co., Inc., Idaho Falls, USA.

Hartanto, D., et al., 2019. Benchmarking the New ENDF/B-VIII.0 Nuclear Data Library for the First Core of Indonesian Multipurpose Research Reactor (RSG-GAS). In: 2019 International Conference on Nuclear Data for Science and Technology (ND2019), Beijing, China.

Hartanto, D., Liem, P.H., 2020. Analysis of the first core of the Indonesian multipurpose research reactor RSG-GAS using the Serpent Monte Carlo Code and the ENDF/B-VIII.0 nuclear data library. Nucl. Eng. Technol. 52 (12), 2725–2732.

Iwamoto, O., et al., 2023. Japanese evaluated nuclear data library version 5: JENDL-5. J. Nucl. Sci. Technol. 60 (1), 1–60.

Iwamoto, O., et al., 2020. Status of JENDL. In: 2019 International Conference on Nuclear Data for Science and Technology (ND2019), Beijing, China.

Kiedrowski, B.C., Brown, F.B., 2013. Adjoint-Based *k*-Eigenvalue Sensitivity Coefficients to Nuclear Data Using Continuous-Energy Monte Carlo. Nucl. Sci. Eng. 174 (3), 227–244.

Liem, P.H., 1995. Science and Technology Agency Internal Report. JAERI, Japan.

Liem, P.H., et al., 1998. Fuel management strategy for the new equilibrium silicide core design of RSG GAS (MPR-30). Nucl. Eng. Des. 180 (3), 207–219.

Liem, P.H., 1998. Monte Carlo calculations on the first criticality of the multipurpose reactor G. A. Siwabessy. Atom Indonesia 24 (2).

Liem, P.H., et al., 2019a. Sensitivity and uncertainty analysis on the first core criticality of the RSG GAS multipurpose research reactor. Prog. Nucl. Energy 114, 46–60.

Liem, P.H., et al., 2019b. Nuclear data sensitivity and uncertainty analyses on the first core criticality of the RSG GAS multipurpose reactor. In: 2019 International Conference on Nuclear Data for Science and Technology (ND2019), Beijing, China.

Liem, P.H., Hartanto, D., 2023. The First Core Criticality Analysis of the RSG GAS Multipurpose Research Reactor Using the Newly Released JENDL-5 Nuclear Data Library. ICNC2023, Sendai, Japan.

Liem, P.H., Sembiring, T.M., 2010. Design of transition cores of RSG GAS (MPR-30) with higher loading silicide fuel. Nucl. Eng. Des. 240 (6), 1433–1442.

Liem, P.H., Sembiring, T.M., 2012. Benchmarking the new JENDL-4.0 library on criticality experiments of a research reactor with oxide LEU (20 w/o) fuel, light water moderator and beryllium reflectors. Ann. Nucl. Energy 44, 58–64.
Nagaya, Y., et al., 2005. MVP/GMVP-II: General Multipurpose Monte Carlo Codes for Neutron and Photon Transport Calculations Based on Continuous Energy and Multigroup Methods. JAERI-1348.
Nagaya, Y., et al., 2016. MVP/GMVP Version 3: general purpose monte carlo codes for neutron and photon transport calculations based on continuous energy and multigroup methods. JAEA-Data/code 2016–2029.
OECD/NEA, 2016. International Handbook of Evaluated Criticality Safety Benchmark Experiments. OECD Nuclear Energy Agency, Paris, France.
OECD/NEA, 2017. International Handbook of Evaluated Reactor Physics Benchmark Experiments. OECD Nuclear Energy Agency, Paris, France.
Rearden, B.T., Jessee, M.A., (Ed.), 2009. Tsunami utility modules. ORNL/TM-2005/39 Version 6, Vol. III, Sect M18.
Rearden, B.T., Jessee, M.A., (Ed.), 2016. SCALE Code System. ORNL/TM-2005/39 Version 6.2.1.
Sembiring, T.M., et al., 2001. Neutronics Design of Mixed Oxide-Silicide Cores for the Core Conversion of RSG-GAS Reactor. Atom Indonesia 27 (2), 85–101.
Shibata, K., et al., 2011. JENDL-4.0: a new library for nuclear science and engineering. J. Nucl. Sci. Technol. 48 (1).
Tada, K., et al., 2023. JENDL-5 benchmarking for fission reactor applications. J. Nucl. Sci. Technol. 2023 https://doi.org/10.1080/00223131.2023.2197439.
Werner, C.J., et al. (Ed.), 2017. MCNP User's Manual; Code Version 6.2. LA-UR-1729981.
Wiarda, D., Dunn, M.E., 2008. PUFF-IV: a code for processing ENDF uncertainty data into multigroup covariance matrices. ORNL/TM-2006/147/R1 (October 2006, Revised 2008).
Wiarda, D., et al., 2016. AMPX-6: A Modular Code System for Processing ENDF/B. ORNL/TM-2016/43.
Wieselquist, W.A., et al., 2021. SCALE 6.3.0 User Manual. ORNL/TM-SCALE-6.3.0.